



# OPTIMAL VIBRATION ESTIMATION OF A NON-LINEAR FLEXIBLE BEAM MOUNTED ON A ROTATING COMPLIANT HUB

A. EL-SINAWI AND M. N. HAMDAN

*Department of Mechanical Engineering, King Fahd University of Petroleum & Minerals, KFUPM Box 1887, Dhahran 31261, Saudi Arabia. E-mail: [elsinawi@kfupm.edu.sa](mailto:elsinawi@kfupm.edu.sa)*

*(Received 22 October 2001, and in final form 22 February 2002)*

To eliminate the need for sensor placement on rotating flexible beams such as turbine blades, helicopter rotors and like applications, a new approach has been developed based on the linear quadratic estimator (LQE) technique for estimating the vibration of any point on the span of a rotating flexible beam mounted on a compliant hub (*plant*) in the presence of process and measurements noise. A non-linear model of the plant is utilized in this study to mimic the actual plant behavior. The corresponding plant dynamics of the LQE are in the form of a reduced order linear model constructed from the eigenvalues and eigenfunctions of a finite element dynamic model of the plant formulated in the state space. A virtual hub deflection (that mimics the actual measurement of the vertical hub deflection needed by the estimation process) is generated by the non-linear model of the plant. The LQE reconstructs the states of the plant, including transverse deflection of the beam at any point, from the measurements of the vertical deflection of the hub, assuming that it is the most accessible state for measurement. Estimated beam tip deflection obtained by the proposed technique is then compared to the tip deflection generated by the non-linear model and the results show good agreement.

© 2002 Elsevier Science Ltd. All rights reserved.

## 1. INTRODUCTION

Rotating flexible beams similar to Figure 1, model turbine blades, helicopter rotors, robot arms and like systems. Extensive studies on the vibration of rotating flexible beams has been dedicated to the development of theoretical models that describe the characteristics of such vibration in a pure mathematical fashion [1–7]. However, few studies have discussed the method by which the vibration of rotating beams could be monitored and/or controlled. Khulief [8] has proposed the control of a rotating beam mounted on a rigid hub using a linear quadratic regulator, which required the placement of the sensor and actuator on the rotating beam. Lee and Eillott [9], Yousefi-Koma and Vukovich [10], Zimmerman and Cudney [11], and Mallory and Miller [12] all have also suggested placing sensors at various locations along the span of the beam for monitoring and control purposes. However, their research has focused on either non-rotating beams or large space structures.

Real-life applications that require in line monitoring and/or control of a rotating beam may face many problems regarding sensor(s) placement on the beam such as high speeds, extreme temperatures, and high centrifugal forces.

Another issue regarding many of the research studies dealing with the monitoring and/or control of vibration of flexible rotating beams is that, they are limited to deterministic

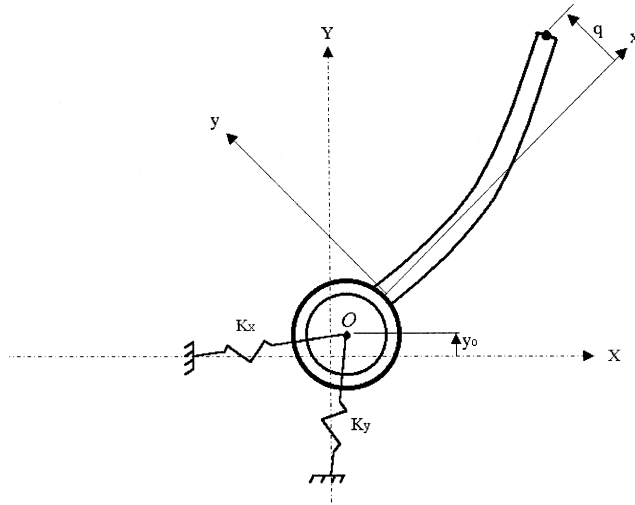


Figure 1. Deflected rotating flexible beam mounted on a compliant hub.

models of the system. In reality, however, components of structural and mechanical systems often exhibit considerable stochastic variations in their properties. Thus, the characteristics of a structure corresponding to these properties show some stochastic variations [13]. This makes it necessary to take account of the uncertainties of system parameters if highly reliable models and/or control schemes are to be utilized.

To eliminate the need for a sensor placement on rotating flexible beam such as turbine blades, helicopter rotors and like applications, a new approach based on the linear quadratic estimator (LQE) technique for estimating the vibration of any point on the span of a rotating flexible beam mounted on a compliant hub and undergoing large planar deformation (plant) and subject to process and measurements noise has been developed. A non-linear model of the plant is utilized to mimic the actual plant behavior [13]. The corresponding plant dynamics of the LQE are in the form of a reduced order linear model constructed from the eigenvalues and eigenfunctions of a finite element dynamic model of the plant and formulated in the state space [6, 14–17]. The LQE reconstructs the states of the plant, including transverse deflection of the beam, from the virtual measurements of the vertical deflection of the hub, which is assumed to be the most accessible state for measurement.

## 2. FINITE ELEMENT MODEL

To implement the proposed scheme on a distributed parameter system such as the beam in Figure 1, the structure is discretized into finite elements forming an  $n$ -dimensional discrete spring–mass–damper system whose dynamics is described by the second order matrix differential equation

$$\mathbf{M}\ddot{\mathbf{x}}(t) + \mathbf{C}\dot{\mathbf{x}}(t) + \mathbf{K}\mathbf{x}(t) = \mathbf{u}(t), \quad (1)$$

where  $\mathbf{M}$ ,  $\mathbf{K}$  and  $\mathbf{C}$  are, respectively, the mass, stiffness, and damping coefficient square, symmetric matrices with their dimensions equal to the number of degrees of freedom  $n$  [18].  $\mathbf{x}(t)$  and  $\mathbf{u}(t)$  are the displacement and force vectors respectively. For systems with

classical damping, i.e., the systems with damping matrix **C** proportional to the mass **M** and stiffness **K** matrices, **M**, **K** and **C** can be diagonalized using normalized orthonormal eigenvectors as the columns of the transformation matrix [15], resulting in

$$\ddot{\eta}_i(t) + 2\zeta_i\omega_i\dot{\eta}_i(t) + \omega_i^2\eta_i(t) = Q_i u(t), \quad i = 1, \dots, n, \tag{2}$$

where  $\eta_i$ ,  $\omega_i$ , and  $\zeta_i$  represent the transformed co-ordinates, natural frequency, and damping ratio of the structure's  $i$ th mode of vibration. When the input is point force (as in the case of actuators),  $Q_i$  is the vector of the  $i$ th eigenfunction evaluated at the force input location.

Using equations (1) and (2) the formulation presented by equations (3) and (4) given below is the basis for state-space modelling of flexible structures, having point force(s) as the input(s) and point displacement(s) as the measured output(s):

$$\dot{\mathbf{z}} = \begin{bmatrix} \mathbf{0} & \mathbf{I} \\ -\mathbf{\Omega}^2 & -2\zeta\mathbf{\Omega} \end{bmatrix} \mathbf{z} + \begin{bmatrix} \mathbf{0} \\ \mathbf{Q} \end{bmatrix} \mathbf{u}, \tag{3}$$

$$\mathbf{y} = [\mathbf{W} \quad \mathbf{0}] \mathbf{z} + \mathbf{D}\mathbf{u}, \tag{4}$$

where

state vector:  $\mathbf{z}(t) = \begin{Bmatrix} \boldsymbol{\eta}(t) \\ \dot{\boldsymbol{\eta}}(t) \end{Bmatrix}$ ,

number of modes:  $N_m$ ,

number of inputs:  $N_u$ ,

number of outputs:  $N_y$ ,

modal displacement:  $\boldsymbol{\eta}(t) = \{\eta_1(t), \eta_2(t), \dots, \eta_{N_m}(t)\}^T$ ,

modal velocity:  $\dot{\boldsymbol{\eta}}(t) = \{\dot{\eta}_1(t), \dot{\eta}_2(t), \dots, \dot{\eta}_{N_m}(t)\}^T$ ,

input:  $\mathbf{u}(t) = \{u_1(t), u_2(t), \dots, u_{N_u}(t)\}^T$ ,

spatial coordinates:  $r_i$ ,

output:  $\mathbf{y}(t) = \{x(r_1, t), x(r_2, t), \dots, x(r_{N_y}, t)\}^T$ ,

natural frequency:  $\mathbf{\Omega} = \text{diag}\{\omega_1, \omega_2, \dots, \omega_{N_m}\}$ ,

modal damping:  $\zeta = \text{diag}\{\zeta_1, \zeta_2, \dots, \zeta_{N_m}\}$ ,

eigenfunction  $i$  at location  $j$ :  $\psi_{ij}$ ,

input matrix:  $\mathbf{Q} = \begin{bmatrix} \psi_{1,1}, & \dots, & \psi_{1,N_u} \\ \vdots & \ddots & \vdots \\ \psi_{N_m,1}, & \dots, & \psi_{N_m,N_u} \end{bmatrix}$ ,

output matrix:  $\mathbf{W} = \begin{bmatrix} \psi_{1,1}, & \dots, & \psi_{N_m,1} \\ \vdots & \ddots & \vdots \\ \psi_{1,N_y}, & \dots, & \psi_{N_m,N_y} \end{bmatrix}$ .

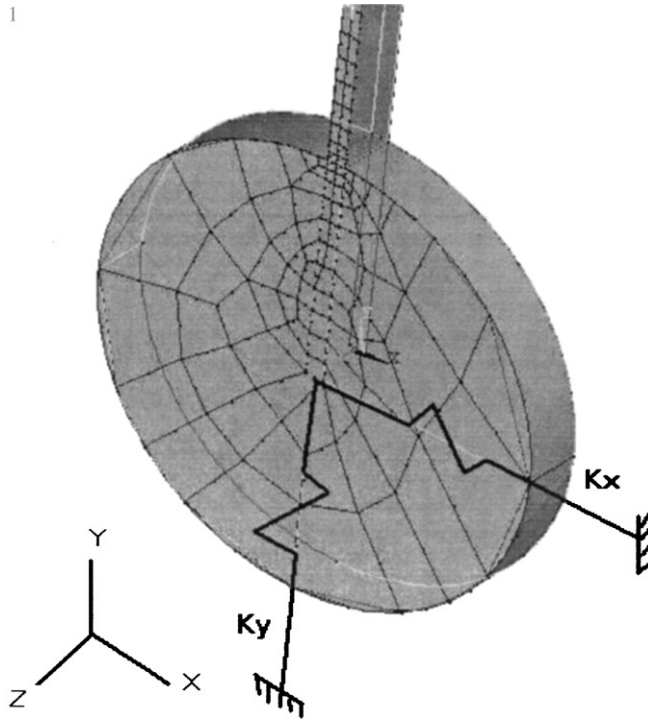


Figure 2. Finite element model of the plant.

The **A**, **B**, **C** and **D** matrices shown in equations (5) and (6), below that describe the state-space model of the flexible structure, are functions of the system (natural frequency, damping ratio, and mode shapes (eigenfunctions)), i.e., if we assume  $\theta = [\omega_i, \zeta_i, \text{ and } \psi_i]_{i=1, \dots, n}$ , then the resulting state-space model format is

$$\dot{\mathbf{z}} = \mathbf{A}(\theta)\mathbf{z} + \mathbf{B}(\theta)\mathbf{u}, \quad (5)$$

$$\mathbf{y} = \mathbf{C}(\theta)\mathbf{z} + \mathbf{D}(\theta)\mathbf{u}. \quad (6)$$

The information needed to construct the **A**, **B**, **C**, and **D** matrices of equations (5) and (6) (i.e., mode shapes and natural frequencies) can be easily obtained by performing finite element analysis on a solid model of the plant using one of the readily available FEA commercial software packages. A portion of the finite element model used to generate the state-space model of the plant is shown in Figure 2.

### 3. OPTIMAL STATE ESTIMATOR (OBSERVER) DESIGN

The first step in designing the proposed optimal estimation technique is the design of the Kalman gains [19, 20]. The plant used for this purpose is the one represented by equations (5) and (6).

A Kalman estimator is used to estimate, on the basis of noisy measurements, the values of the state variables of a system subject to stochastic input–output disturbances. The input disturbances are included in the state-space model by adding the noise input vector  $v$  to the exogenous input vector  $u$ . Moreover, to include measurement noise, the vector  $w$  is

added to the output of the system. Such noise signals are usually part of the actual mode of the system.

The Kalman estimator takes on a particularly simple structure closely resembling the original system [19, 20]. The state-space model of the Kalman estimator is expressed by the following equation:

$$\dot{\hat{\mathbf{y}}} = \mathbf{A}\hat{\mathbf{y}} + \mathbf{L}[\tilde{\mathbf{y}} - \mathbf{C}\hat{\mathbf{y}}] + \mathbf{B}\mathbf{u} \tag{7}$$

and

$$\mathbf{L} = \mathbf{S}_0\mathbf{C}^T\mathbf{R}^{-1}, \tag{8}$$

where  $\hat{\mathbf{y}}$  is the vector of the state estimates,  $\tilde{\mathbf{y}}$  is the vector of measured states from the actual system,  $\mathbf{L}$  is the Kalman matrix of gains, and  $\mathbf{S}_0$  is the steady state solution of the following matrix *Riccati* differential equation [18–20]:

$$\dot{\mathbf{S}} = \mathbf{A}\mathbf{S} + \mathbf{S}\mathbf{A}^T - \mathbf{S}\mathbf{C}^T\mathbf{R}^{-1}\mathbf{C}\mathbf{S} + \mathbf{B}\mathbf{Q}\mathbf{B}^T. \tag{9}$$

Matrices  $\mathbf{R}$  and  $\mathbf{Q}$  are the symmetric, non-negative matrices that minimizes the following performance index  $J$ :

$$J = \int_0^\infty (\mathbf{x}^T\mathbf{B}\mathbf{Q}\mathbf{B}^T\mathbf{x} + \mathbf{u}^T\mathbf{R}\mathbf{u}) dt. \tag{10}$$

It is worth mentioning that knowledge of the absolute magnitude of  $\mathbf{R}$  and  $\mathbf{Q}$  is not important, rather, only their relative magnitude is important [15, 20].

Now, with the linear time-invariant model of the system available, namely equations (5) and (6), along with the Kalman matrix of gains  $\mathbf{L}$ , optimal estimates of the plant states can be obtained according to equation (7).

It is worth mentioning that the controllability and observability of the estimator are found by obtaining the rank of their corresponding gramians. Full-rank gramians indicate a controllable and observable system [15, 20, 21]. The proposed estimation scheme is shown in Figure 3.

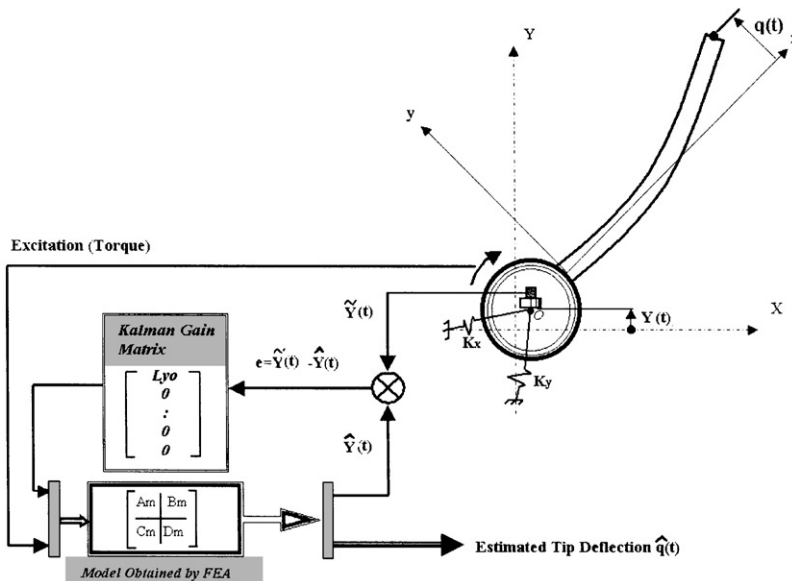


Figure 3. Schematic of the proposed LQE approach for estimating beam tip deflection.

## 4. NON-LINEAR MODEL OF THE BEAM-HUB SYSTEM (PLANT)

A mathematical model for a flexible beam undergoing large planar flexural deformations, continuously rotating under the effect of hub torque and mounted on a compliant hub has been developed by Al-Bedoor *et al.* [13]. Lagrangian dynamics in conjunction with the assumed modes method were utilized to derive, directly, the non-linear equivalent temporal equations of motion. The following four coupled non-linear ordinary differential equations represent the generated non-linear mathematical model:

$$\begin{aligned} (1 + \mu)\ddot{X} + \frac{1}{2}[(1 + 2C + b_3q^2)\sin\theta - 2b_1q\cos\theta]\ddot{\theta} \\ + \frac{1}{2}[(1 + 2C + b_3q^2)\cos\theta + 2b_1q\sin\theta]\dot{\theta}^2 \\ + 2[b_3q\sin\theta - b_1\cos\theta]\dot{q}\dot{\theta} - (b_3\cos\theta)\dot{q}^2 \\ - [b_1\sin\theta + b_3q\cos\theta]\ddot{q} + \beta s_1^2 X = F_X, \end{aligned} \quad (11)$$

$$\begin{aligned} (1 + \mu)\ddot{Y} + \frac{1}{2}[(1 + 2C - b_3q^2)\cos\theta - 2b_1q\sin\theta]\ddot{\theta} \\ - \frac{1}{2}[(1 + 2C - b_3q^2)\sin\theta + 2b_1q\cos\theta]\dot{\theta}^2 \\ - 2[b_3q\cos\theta + b_1\sin\theta]\dot{q}\dot{\theta} - (b_3\sin\theta)\dot{q}^2 \\ + [b_1\cos\theta - b_3q\sin\theta]\ddot{q} + \beta s_2^2 Y = F_Y, \end{aligned} \quad (12)$$

$$\begin{aligned} [b_0 + b_{12}q_i^2]\ddot{\theta} + 2b_{12}q\dot{q}\dot{\theta} + \frac{1}{2}[(1 + 2C + b_3q^2)\sin\theta - 2b_1q\cos\theta]\ddot{X} \\ + \frac{1}{2}[(1 + 2C - b_3q^2)\cos\theta - 2b_1q\sin\theta]\ddot{Y} \\ + \frac{1}{2}[b_{14} + b_7q^2]\ddot{q} + b_7q\dot{q}^2 = \frac{T}{m_B l^2}, \end{aligned} \quad (13)$$

$$\begin{aligned} (b_2 + b_8q^2)\ddot{q} + \frac{1}{2}(b_{14} + b_7q^2)\ddot{\theta} + b_8q\dot{q}^2 \\ - (b_1\sin\theta + b_3q\cos\theta)\ddot{X} \\ + (b_1\cos\theta - b_3q\sin\theta)\ddot{Y} \\ - (2b_{13}q^3 + b_{12}q)\dot{\theta}^2 + \beta^2 b_9q + 2\beta^2 b_1q^3 = 0, \end{aligned} \quad (14)$$

where  $X$  and  $Y$  are the hub horizontal and vertical deflections respectively.  $\theta$  is the rigid-body rotation and  $q$  is the beam  $i$ th modal degree of freedom. The base flexibility is defined as a ratio to the beam flexibility using the parameters  $s_1 = K_X l^3 / EI$  and  $s_2 = K_Y l^3 / EI$ . For more information on the non-linear model see references [13, 14].

## 5. NUMERICAL SIMULATION AND RESULTS

The proposed technique is used to estimate the tip deflection of a beam mounted on a compliant hub and rotating at a constant angular speed of 2400 r.p.m. and subject to external torque is considered. Dimensions and material properties of the beam hub system used in the non-linear model are given in Table 1. This model, as mentioned before, is assumed to be a representation of the actual model. Of course, this model is needed to generate what is assumed to be the measurable states of the actual system, i.e., the vertical hub deflection as shown in Figure 3.

States of the system are generated by numerically integrating equations (11)–(14) using Matlab<sup>®</sup>.

The reduced order linear elastodynamic model of the beam-hub system, i.e. (plant), needed for the construction of the LQE and the corresponding Kalman gains matrix  $L$  is

TABLE 1

*Simulation data for the beam-hub system*

Item	Value
Beam length	3 m
Beam's mass/unit length	6.44 kg/m
Beam's flexural rigidity	3614
Hub radius	0.2 m
Hub mass	50 kg
Hub stiffness	$K_X = K_Y = 1e6$ N/m
Torque applied	40 N m at 5 Hz square wave 1 N m at 20 Hz sine wave

TABLE 2

*Modal frequencies generated by FEA*

Mode	Modal Frequency (Hz)
First mode	6.1183
Second mode	17.191
Third mode	34.745
Fourth mode	61.704

generated from the eigenvalues and eigenfunctions of the finite element model according to equations (5) and (6). The finite element model generated the natural frequencies and mode shapes from the dynamic solution of a solid model of the plant discretized by 162 8-node shell elements each having a thickness equal to the beam-hub depth. The linear state-space model of the plant is then constructed from the first four modes of vibration predicted by the FEA method. The natural frequencies of the first four modes are listed in Table 2. Figure 4 shows the first mode of vibration of the beam-hub system as predicted by finite element analysis.

Modal damping of 1% has been added to the system (assuming natural material damping). Thus the damping matrix  $\mathbf{C}$  is constructed based on the initial assumption that  $\mathbf{C}$  is proportional to the mass and stiffness matrices namely,  $\mathbf{M}$  and  $\mathbf{K}$ .

With the matrices  $\mathbf{A}$ ,  $\mathbf{B}$ , and  $\mathbf{C}$  now available from the finite element model, the Kalman matrix of gains  $\mathbf{L}$  is obtained by solving equations (8)–(10), and the LQE is implemented to estimate the tip deflection of the beam for the first four modes of vibration.

Simulation of the proposed technique is carried out using two types of torque excitation. The first type is a 5 Hz square wave torque with an amplitude of 40 N m and added to it a  $\pm 10$  N m random torque. The second type is a 20 Hz sine wave torque with an amplitude of 1 N m and added to it a  $\pm 1$  N m random torque. The purpose of adding a random torque profile is to simulate process noise. Both excitations are shown in Figures 5 and 6 respectively.

A random signal was added to the virtual measurements of the vertical hub deflection (output of the non-linear model) to simulate measurements noise. Estimates of the transverse beam tip deflection are obtained by plotting the corresponding state estimate generated by the LQE.

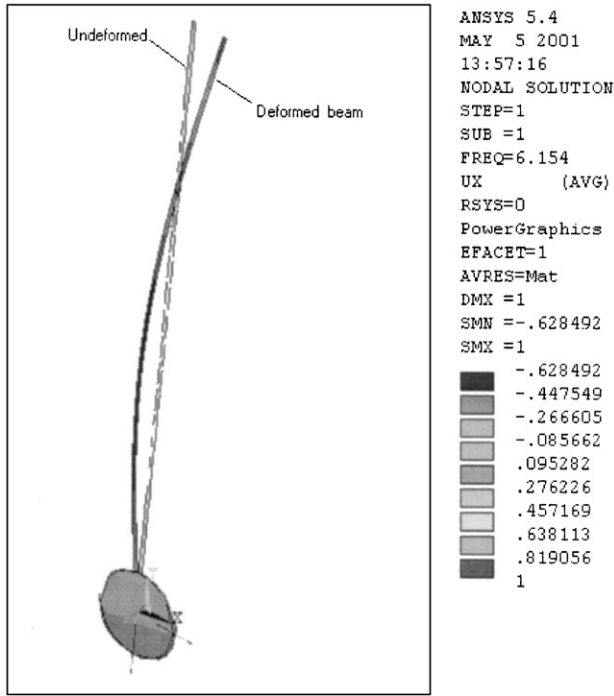


Figure 4. First mode deformation of the beam-hub system as predicted by FEA.

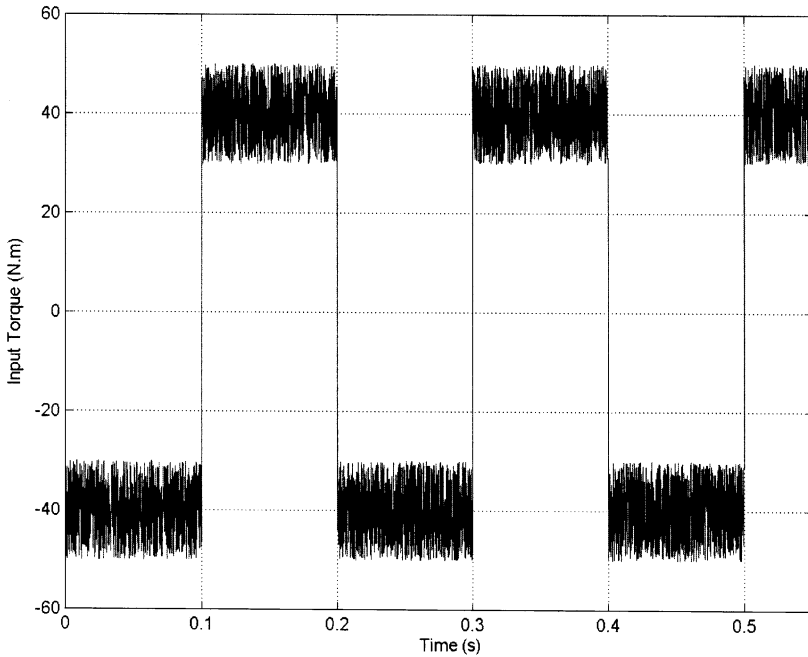


Figure 5. Five Hertz square wave torque profile with added random torque.



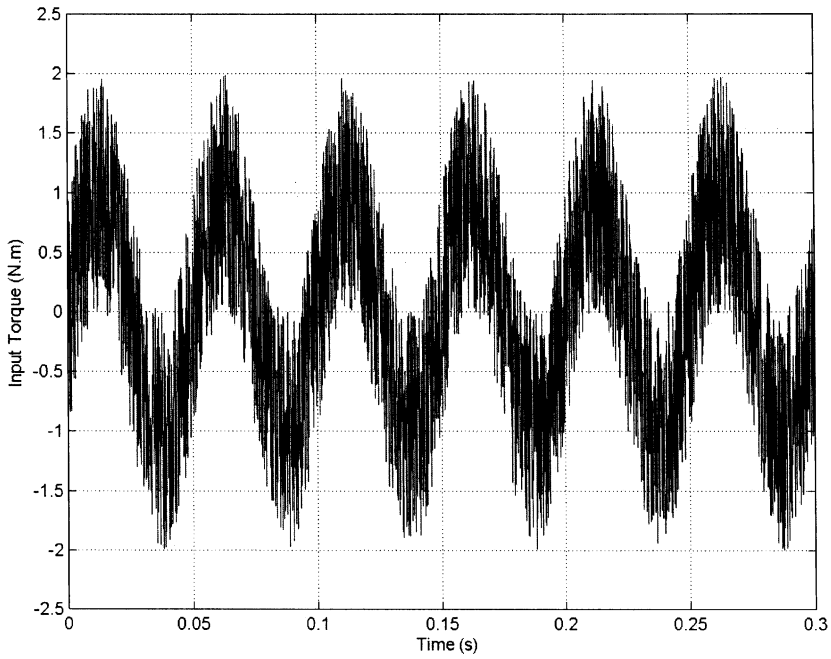


Figure 6. Twenty Hertz sine wave torque profile with added random torque.

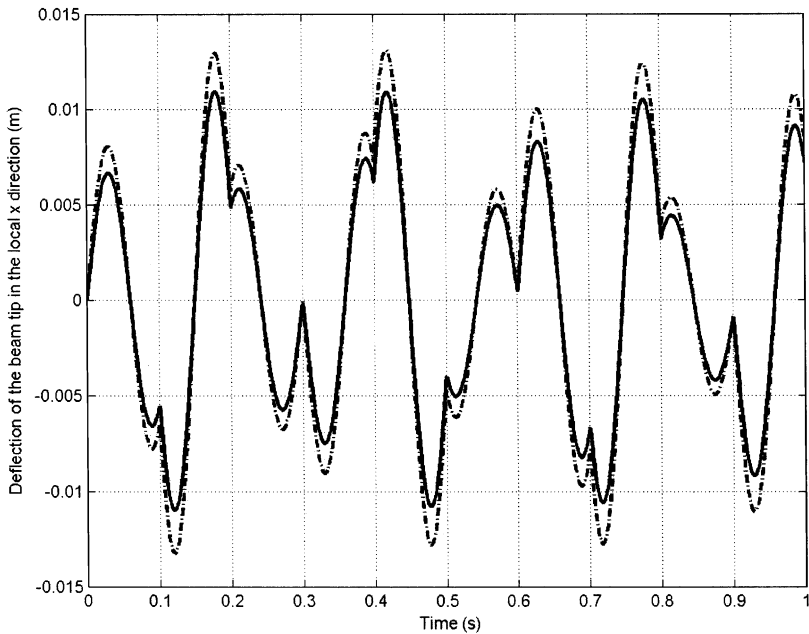


Figure 7. Estimated versus non-linear beam tip deflection (first mode, square wave excitation). — Estimated, - - - - - Actual.

Figures 7–10 show the estimated beam tip deflection compared to the assumed tip deflection (tip deflection predicted by the non-linear model) for the first four modes of vibration when the plant is excited by the 5 Hz square wave torque.

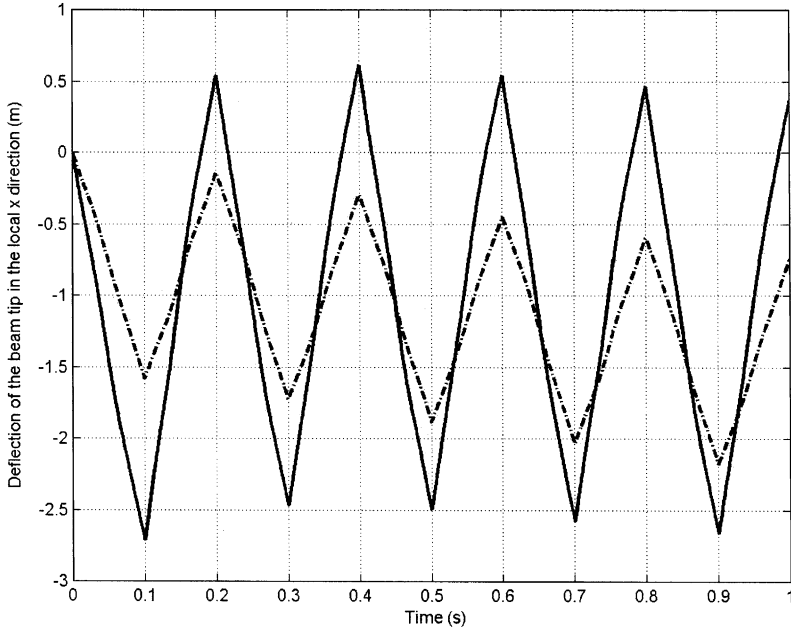


Figure 8. Estimated versus non-linear beam tip deflection (second mode, square wave excitation). — Estimated, - - - - - Actual.

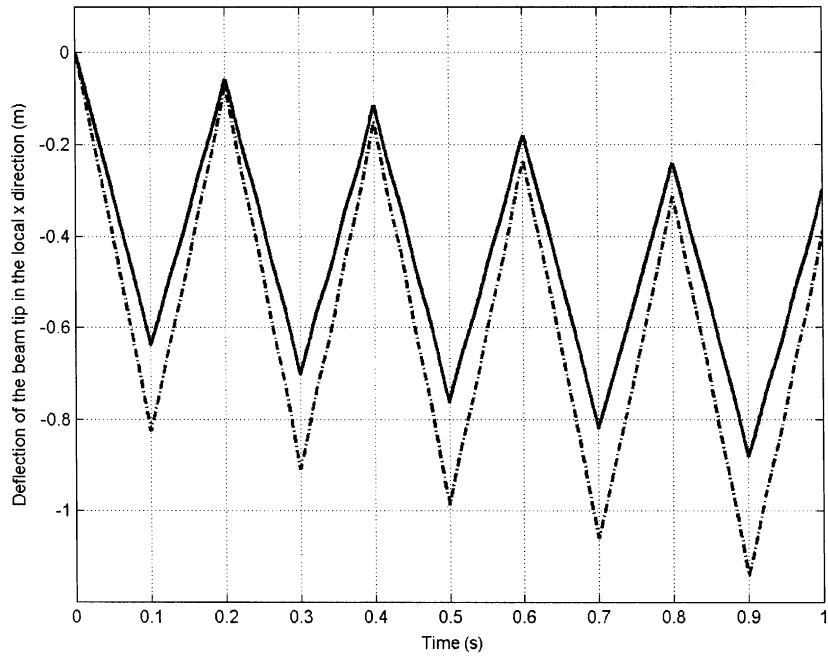


Figure 9. Estimated versus non-linear beam tip deflection (third mode, square wave excitation). — Estimated, - - - - - Actual.

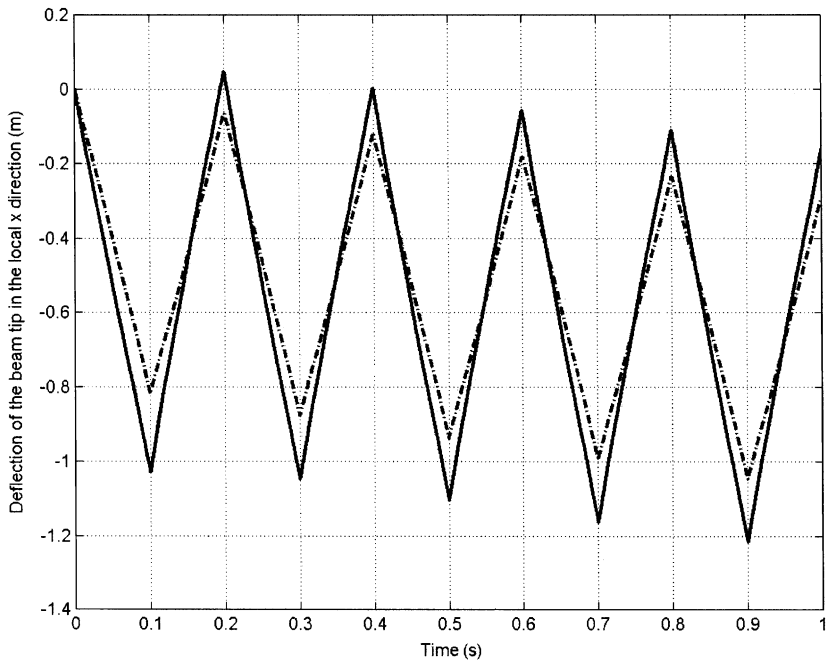


Figure 10. Estimated versus non-linear beam tip deflection (fourth mode, square wave excitation). — Estimated, - - - - - Actual.

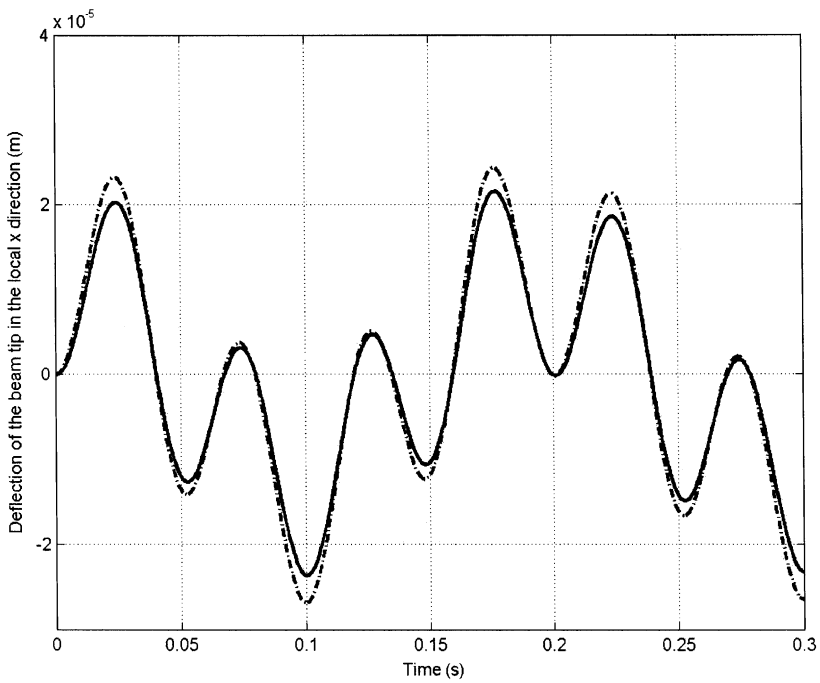


Figure 11. Estimated versus non-linear beam tip deflection (first mode, sine wave excitation). — estimated, - - - - - Actual.

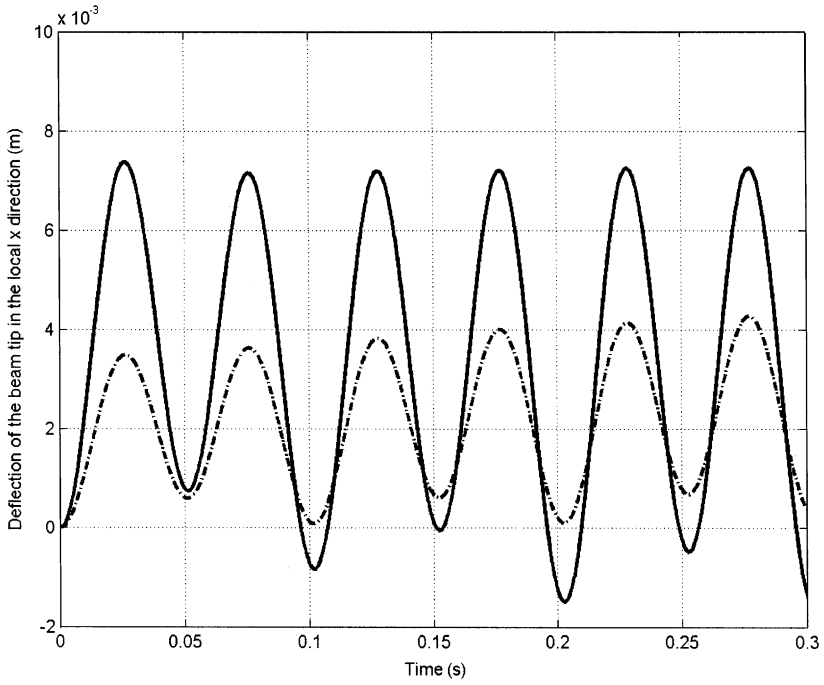


Figure 12. Estimated versus non-linear beam tip deflection (second mode, sine wave excitation). ——— estimated, - - - - - Actual.

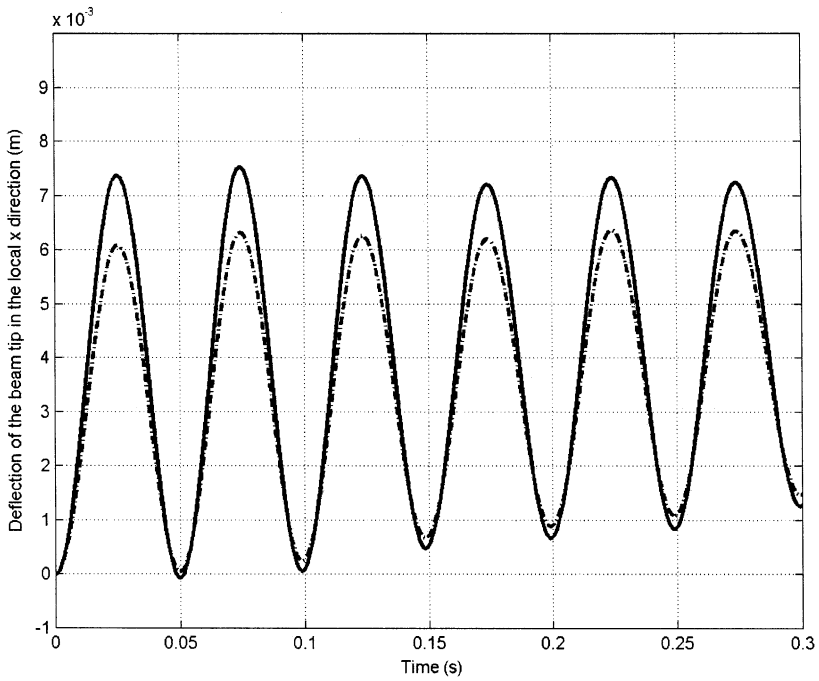


Figure 13. Estimated versus non-linear beam tip deflection (third mode, sine wave excitation). ——— estimated, - - - - - Actual.

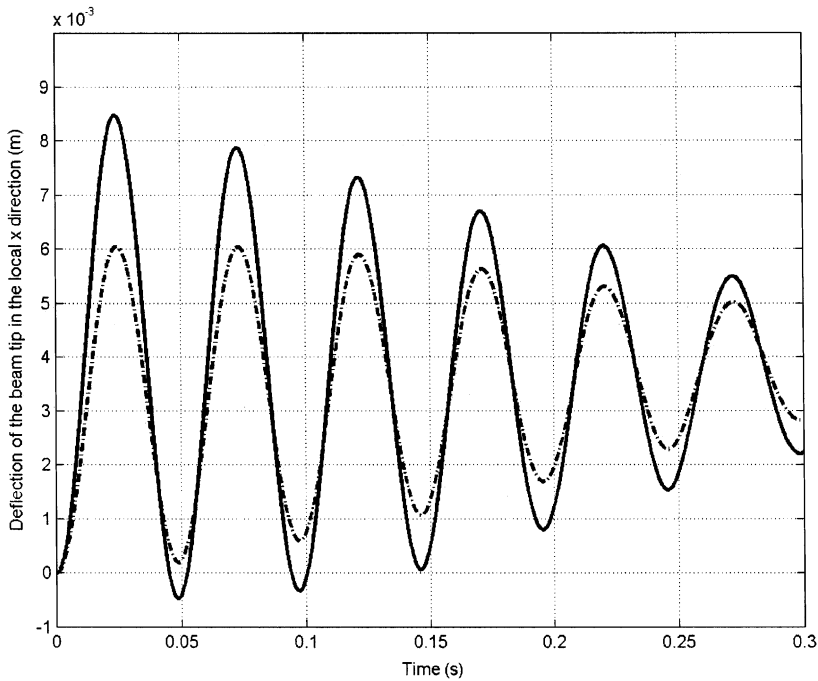


Figure 14. Estimated versus non-linear beam tip deflection (fourth mode, sine wave excitation). ——— estimated, - - - - - Actual.

Figures 11–14 show the similar comparison between estimated tip deflection and the one generated by non-linear when the plant is excited by the 20 Hz sine wave torque profile.

## 6. CONCLUSIONS

A new approach for estimating beam tip deflection via measurements of hub deflection using a linear quadratic estimator for a rotating beam mounted on a compliant hub is presented. A readily available non-linear model is used to mimic the actual vibration of the beam–hub system. Approximate reduced order linear model of the beam–hub system is obtained using finite element analysis.

A linear quadratic estimator is formulated based on the reduced order linear model dynamics and the optimal Kalman matrix of gains is determined from the steady state solution of a matrix Riccati differential equation.

With a fully functional estimator available, measurements of the vertical hub deflection is compared to the estimated hub deflection and the difference (error) is multiplied by the corresponding Kalman gain and fed back to the estimator as a second input. The output of the estimator is a vector of two states, namely, hub deflection and beam tip deflection.

Estimated beam tip deflection is plotted and compared to the tip deflection produced by the non-linear model; see Figures 7–14. Simulation results show that the proposed approach is capable of producing fairly accurate estimates of the tip deflection for most modes. However, over estimates of the tip deflection for some modes have persisted

especially for the second mode (Figures 8 and 12). The authors have not yet been able to justify such discrepancy.

#### ACKNOWLEDGMENTS

Authors would like to thank King Fahd University of Petroleum and Minerals and the University of Jordan for their continuous support.

#### REFERENCES

1. W. D. ZHU and C. D. MOTE JR. 1997 *Journal of Dynamic Systems Measurements and control* **119**, 802–808. Dynamic modeling and optimal control of rotating Euler–Bernolli beams.
2. F. L. HU and A. G. ULSOY 1994 *Journal of Dynamic Systems Measurements and Control* **116**, 56–65. Dynamic modeling of constrained flexible robot arm for controller design.
3. T. ZHENG and N. HAEBE 2000. *Journal of Applied Mechanics* **57**, 485–495, Nonlinear dynamic behavior of a complex rotor-bearing system.
4. T. P. MITCHELL and J. C. BRUCH JR. 1988 *Journal of Vibration, Acoustics, Stress, and Reliability Design* **110**, 18–120. Free vibration of a flexible arm attached to a compliant finite hub.
5. M. SWAMINADHAM and M. CHINTA 1994 *Journal of Sound and Vibration* **174**, 284–288. Vibration of a turbo machine blade with flexible root.
6. A. BAZOUNE, Y. A. KHULIEF, N. G. SZEPHEN and M. A. MOHIUDDIN 2001 *Finite Element in Analysis and Design* **37**, 199–219. Dynamic response of spinning tapered Timoshenko beams using modal reduction.
7. T. R. KANE, R. R. RAYAN and A. K. BANERJEE 1987 *Journal of Guidance* **10**, 139–150. Dynamics of a cantilever beam attached to a moving base.
8. Y. A. KHULIEF 2000 *Journal of Sound and Vibration* **242**, 681–699. Vibration suppression in rotating beams using active modal control.
9. Y. S. LEE and S. J. ELLIOTT 2001 *Journal of Sound and Vibration* **242**, 767–791. Active position control of flexible smart beam using internal model control.
10. A. YOUSEFI-KOMA and G. VUKOVICH 2000 *Journal of Guidance, Control, and Dynamics* **23**, 347–354. Vibration suppression of flexible beams with bonded piezo transducers using wave-absorbing controllers.
11. D. C. ZIMMERMAN and H. H. CUDNEY 1989 *Journal of Vibration, Acoustics, Stress, and Reliability in Design* **111**, 283–289. Practical implementation issues for active control of large flexible structures.
12. W. MALLORY and D. W. MILLER 2000 *Journal of Guidance, Control, and Dynamics* **23**, 665–672. Decentralized state estimation for flexible space structures.
13. B. AL-BEDDOOR, A. EL-SINAWI, and M. N. HAMDAN 2002 *Journal of Sound and Vibration* **251**, 767–781. Non-linear dynamic model of an inextensible rotating flexible arm. Supported on a flexible base.
14. A. EL-SINAWI, B. AL-BEDDOOR and M.N. HAMDAN July 2001 *Proceedings of the ASME PVP Conference in Atlanta, Georgia*. Non-linear dynamic model of an inextensible rotating flexible beam supported on a flexible base.
15. A. EL-SINAWI and A. R. KASHANI 2001 *Journal of Vibration and Control* **7**, 1163–1173. Active isolation using a Kalman estimator-based controller.
16. A. EL-SINAWI and A. R. KASHANI 1999 *Society of Automotive Engineers*, Paper No. 1999-01-1845. Active control of engine mounts.
17. A. EL-SINAWI and A. R. KASHANI. 1999 *Proceedings of the International Mechanical Engineering Conference and Exposition, Anaheim, CA*. Active vibration isolation of a plate.
18. W. GAWRONSKI and T. WILLIAMS 1991 *Journal of Guidance* **4**, 68–76. Modal reduction for flexible space structures.
19. R. E. KALMAN and R. S. BUCY 1961 *Journal of Basic Engineering* 95–101. New results in linear filtering and prediction theory.
20. B. HASSIBI, A. H. SAYED and T. KAILATH 1999 *Indefinite-Quadratic Estimation and Control*. Philadelphia, PA: SIAM Publications.

21. R. E. KALMAN 1960 *Journal of Basic Engineering Volume No?* 35–45. A new approach to linear filtering and prediction problems.

APPENDIX A: COEFFICIENTS OF THE NON-LINEAR INEXTENSIBLE BEAM MODEL

$$\begin{aligned}
 b_1 &= \int_0^1 \phi^2 d\xi, & b_2 &= \int_0^1 \phi^2 d\xi = 1, & b_3 &= \frac{1}{4} \left[ \int_0^1 \left[ \int_0^\xi \phi'^2 d\gamma \right] \right] d\xi, \\
 b_4 &= \int_0^1 \xi \left[ \int_0^\xi \phi'^2 d\gamma \right] d\xi, & b_5 &= \int_0^1 \left[ \int_0^\xi \phi'^4 d\gamma \right] d\xi, & b_6 &= \int_0^1 \xi \left[ \int_0^\xi \phi'^4 d\gamma \right] d\xi, \\
 b_7 &= \int_0^1 \phi \left[ \int_0^\xi \phi'^2 d\gamma \right] d\xi, & b_8 &= \int_0^1 \left[ \int_0^\xi \phi'^2 d\gamma \right]^2 d\xi, & b_9 &= \int_0^1 \phi^2 d\xi, \\
 b_{10} &= \int_0^1 (\phi' \phi'')^2 d\xi, & b_{11} &= \int_0^1 \xi \phi d\xi, \\
 b_{12} &= b_2 - cb_3 - b_4, & b_{13} &= \frac{1}{4}(b_8 - b_6 - cb_5), & b_{14} &= 2cb_1 = 2b_{11},
 \end{aligned}$$

where the prime indicates a derivative with respect to the dimensionless parameter,  $\xi$ .

The parameters  $\xi$  and  $\gamma$  are related to the inextensibility condition that dictates the total axial shortening  $u(s, t)$  according to the following equation [25]:

$$\lambda u(\xi, t) = \xi - \int_0^\xi \cos \psi(\gamma, t) d\gamma,$$

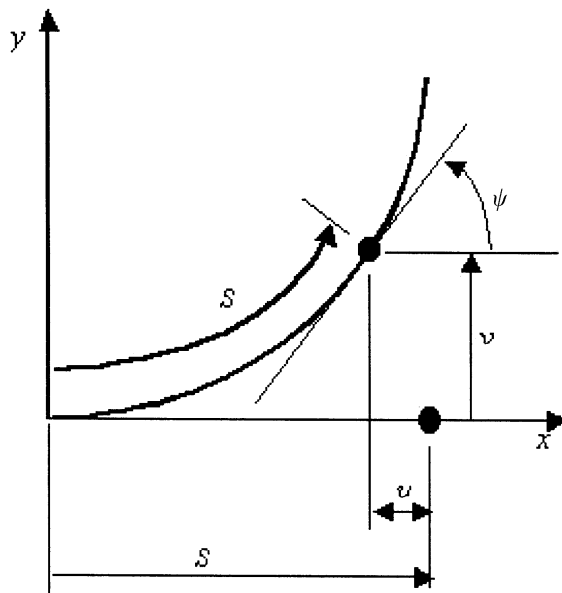


Figure 15. Deformed beam configuration.

where the dimensionless parameter  $\xi = s/l$ ,  $s$  is the distance between a point on the beam and the root of the beam,  $l$  is the length of the beam (see Figure A1),  $\lambda = 1/l$ , and  $\phi_i$  is the mode shape of the cantilever beam which is expressed in the form:

$$\phi_i(\xi) = \left(\frac{1}{r_i}\right) [\cosh p_i \xi - \cos p_i \xi - \alpha_i (\sinh p_i \xi - \sin p_i \xi)],$$

where  $r_i = |\phi_i(\xi)|_{max}$  is a scaling factor,  $p_i = m_b \omega_{ni} l^3 / EI$  ( $\omega_{ni}$  is the  $i$ th modal frequency of the non-rotating linear cantilever beam) is the  $i$ th dimensionless frequency parameter found from the solution of the transcendental frequency equation

$$\cos p_i \cosh p_i + 1 = 0$$

and  $\alpha_i$  is a weighting constant associated with each mode, defined as

$$\alpha_i = \frac{(\sinh p_i - \sin p_i)}{(\cosh p_i + \cos p_i)}.$$